

# Influence of molecular vibrations on dissociative adsorption

Axel Gross and Matthias Scheffler

*Fritz-Haber-Institut der Max-Planck-Gesellschaft, Faradayweg 4-6, D-14195 Berlin-Dahlem,  
Germany*

## Abstract

The influence of molecular vibrations on dissociative adsorption is studied by six-dimensional quantum dynamical calculations. For the system H<sub>2</sub> at Pd (100), which possesses non-activated pathways, it is shown that large vibrational effects exist and that they are not due to a strongly curved reaction path and a late dissociation-hindering minimum barrier, as was previously assumed. Instead, they are caused by the lowering of the H-H vibrational frequency during the dissociation and the multi-dimensionality of the potential energy surface. Still there are quantitative discrepancies between theory and experiment identified.

## I. INTRODUCTION

In recent years the dissociative adsorption and associative desorption of hydrogen on metal surfaces has been the subject of many experimental and theoretical investigations (see, e.g., Refs. [1,2,3] and references therein). The studies were motivated by the fact that for these relatively simple systems the process of bond breaking and bond making during dissociative adsorption can be analyzed in greater detail.

Breaking a molecular bond is obviously coupled to the interatomic distance and molecular vibrations. Therefore a large number of studies have addressed the influence of those vibrations on the dissociative adsorption and associative desorption, especially in the benchmark system  $H_2/Cu$  [4,5,6,7,8,9]. In desorption studies [4,5] strong vibrational heating of the hydrogen molecules was found, i.e., vibrational population ratios were much greater than expected for thermal equilibrium with the temperature of the substrate at which desorption occurs. According to the principle of microscopic reversibility this implies that the probability of dissociative adsorption should be enhanced for vibrational excited molecules, which indeed has been confirmed experimentally [6,7,8,9]. These vibrational effects were usually discussed [10,11,12,13] within the context of potential energy surfaces (PESs) which depend only on two coordinates, namely the center of mass distance of the molecule from the surface,  $Z$ , and the H-H interatomic distance,  $d$ . Obviously, the motion of the two atoms of a diatomic molecule is governed by six coordinates, not just  $Z$  and  $d$ , but the dependence on the other (neglected) four coordinates was felt to be of minor importance. It was generally accepted that the PES in the considered two-dimensional space (a so-called “elbow plot”) should exhibit a strongly curved reaction path and a so-called late barrier towards dissociative adsorption, i.e. a barrier after the curved region of the PES, close to the surface, in order to account for strong vibrational effects in dissociative adsorption and associative desorption.

Interestingly, strong vibrational heating was also found for hydrogen molecules desorbing from Pd (100) [14], although for this substrate, in contrast to Cu, the dissociative adsorption

is non-activated [15,16,17]. Nevertheless, within the spirit of the above discussion for the H<sub>2</sub>/Cu system, Brenig *et al.* [18,19] reproduced the vibrational heating for H<sub>2</sub> desorption from Pd (100) by quantum dynamical calculations using two-dimensional model potentials with a minimum barrier of 200 meV. Since this is in conflict with the fact that adsorption of H<sub>2</sub> in non-activated, Darling and Holloway [20,21] questioned the validity of this theoretical work and argued that one has to take into account a distribution of barrier heights which requires higher-dimensional calculations. In their model calculations, which were still two-dimensional, they basically showed that it is not possible to reproduce vibrational heating in desorption with a barrier-less two-dimensional elbow potential [20].

Recently we enhanced the computational approach for scattering of molecules at surfaces [19,22] and are now able to investigate reactions of diatomic molecules on surfaces with all six degrees of freedom of the molecule being treated quantum dynamically [23]. Such a study was performed for the sticking probability of H<sub>2</sub> at Pd (100) [23] employing a high-dimensional PES derived from first-principles calculations [17]. In the present paper we use the same PES and the same six-dimensional (6-D) quantum-dynamical method. The PES for the interaction of H<sub>2</sub> and Pd (100) possesses non-activated pathway, but also (in fact in majority) activated pathways [17]. It was found that H<sub>2</sub> molecules impinging with small energies are efficiently steered along the non-activated pathways towards dissociative adsorption [23]. However, with increasing energy the steering effect gets less effective and the majority of molecules proceeds via pathways with energy barriers [23]. The steering mechanism is operative for the translational degree of freedom as well as for the rotations [24]. In the meantime two predictions of the quantum dynamical calculations for H<sub>2</sub>/Pd (100), namely the strong rotational hindering of the dissociation at low kinetic energy [23,25] and the orientation dependence of adsorption and desorption [23], have been confirmed experimentally [26,27].

In order to investigate the effects of molecular vibrations on the sticking probability we had to extend the calculations [23] to higher energies. To describe the dynamics of initially vibrating molecules properly we have increased the number of vibrational eigenfunctions in

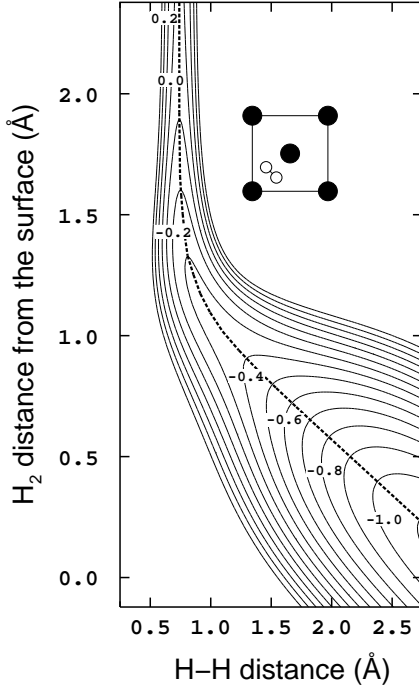


FIG. 1. Contour plot of the PES along a two-dimensional cut through the six-dimensional coordinate space of  $\text{H}_2/\text{Pd}(100)$ . The inset shows the orientation of the molecular axis and the lateral  $\text{H}_2$  center-of-mass coordinates. The coordinates in the figure are the  $\text{H}_2$  center-of-mass distance from the surface  $Z$  and the H-H interatomic distance  $d$ . The dashed line is the optimum reaction path. Energies are in eV per  $\text{H}_2$  molecule. The contour spacing is 0.1 eV.

the expansion of the wave function of the hydrogen nuclei: In the present study up to 25,200 channels per total energy are taken into account compared to 21,000 channels which were considered previously [23]. We will show that in spite of the absence of a minimum barrier towards dissociative adsorption and a strongly curved reaction path there are still substantial vibrational effects in the adsorption and desorption of  $\text{H}_2/\text{Pd}(100)$ . We will demonstrate that they are caused by a strong lowering of the H-H vibrational frequency during the adsorption and by the multi-dimensionality of the PES relevant for the dissociation process. However, some discrepancies to the experimental results of refs. [14,18] remain.

## II. RESULTS AND DISCUSSION

Figure 1 shows a cut through our PES of  $\text{H}_2/\text{Pd}(100)$ , where the most favorable path

towards dissociative adsorption is marked by the dashed line. As discussed above, for this path there is no energy barrier hindering dissociation, i.e., the adsorption is non-activated. The curvature of the optimum reaction pathway (see dashed line in Fig. 1) is relatively moderate compared to the curvature of reaction pathways of previously assumed or guessed PESs which had been used in earlier low-dimensional studies [10,11,12,13,18,19,20]. The detailed total-energy calculations [17] showed that the PES is strongly anisotropic and corrugated so that besides non-activated paths the majority of pathways towards dissociative adsorption has in fact energy barriers with a rather broad distribution of heights and positions. The barrier height depends on the molecular orientation and impact site in the surface unit cell.

Figure 2 presents results for the sticking probability as a function of the kinetic energy of a  $\text{H}_2$  beam under normal incidence. Quantum mechanically determined sticking probabilities for hydrogen at surfaces with an attractive well exhibit an oscillatory structure as a function of the incident energy [23,24,28,29], reflecting the opening of new scattering channels and resonances [28,29], as also observed in, e.g, LEED [30]. Such oscillations have not been observed yet. In the experiments the molecular beams are not strictly mono-energetic but have a certain energetic broadening. For the calculations of Fig. 2 we assumed an energy width  $\Delta E_i/E_i = 0.2$ , typical for experiments [15]. As a consequence, the quantum dynamical oscillations are smoothed out.

The solid curves correspond to 6-D calculations for  $\text{H}_2$  molecules initially in the vibrational ground and first excited state, respectively. The  $\nu_i = 0$  curve shows the characteristic initial decrease of the sticking probability with increasing energy (for  $E_i \lesssim 0.1$  eV) which is due to the decreasing importance of the steering effect with increasing energy [23]. Also for molecules initially in the first excited vibrational state a corresponding behavior is found, but for these the steering effect is strong only for very small energies ( $E_i \lesssim 50$  meV). For kinetic energies higher than  $\approx 50$  meV the  $\nu_i = 1$  molecules experience an increasing sticking probability which is significantly larger than for  $\nu_i = 0$  molecules.

The effect of the initial vibrational state can be quantified by the vibrational efficacy

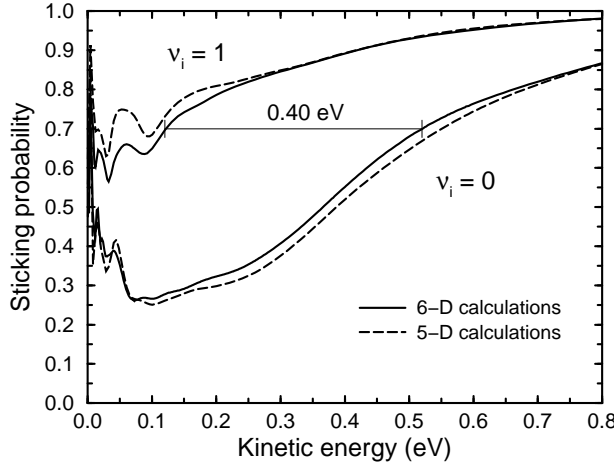


FIG. 2. Sticking probability versus kinetic energy for a  $\text{H}_2$  beam under normal incidence on a Pd(100) surface. The molecules are initially in the rotational ground state  $j_i = 0$ , and in their initial vibrational states are  $\nu_i = 0$  (lower curves) and  $\nu_i = 1$  (upper curves). The solid lines show the results of the 6-D calculations and the dashed lines are five-dimensional calculations where the vibrational degree of freedom is approximated by an adiabatic treatment (see text).

$$\Xi_{\text{vib}}(S) = \frac{\epsilon_{\nu_i=0}(S) - \epsilon_{\nu_i=1}(S)}{\hbar\omega_{\text{vib}}}, \quad (1)$$

where  $\epsilon(S)$  is the kinetic energy required to obtain the sticking probability  $S$ , so that  $\Xi_{\text{vib}}(S)$  is the separation of the sticking curves for a certain sticking probability divided by the gas-phase vibrational quantum  $\hbar\omega_{\text{vib}} = 516$  meV. In Fig. 2 we have marked  $S = 0.7$ , which leads to a value of the vibrational efficacy of  $\Xi_{\text{vib}}(S = 0.7) = 0.75$ . This means that 75% of the vibrational energy is effective in promoting the dissociative adsorption, a value even higher than in the  $\text{H}_2/\text{Cu}(111)$  system [9].

To clarify why and how molecular vibrations effect the sticking probability we performed calculations for a reduced coordinate space, namely allowing only for five degrees of freedom for the two hydrogen atoms. This reduction was achieved by keeping the molecules in their initial vibrational state. Although the vibrational state is kept fixed, the energy of the vibration, which is determined by the strength of the H-H interaction, will change along the scattering pathway. As can be seen in Fig. 2, these five-dimensional results are very close to

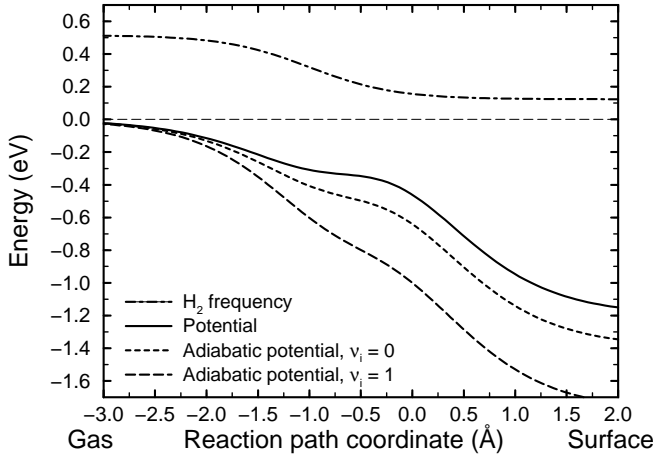


FIG. 3. H-H vibrational frequency  $\hbar\omega(s)$ , potential  $V_0(s)$  and “vibrationally adiabatic potentials” (see Eq. 2) along the reaction path of Fig. 1.  $s = 0$  corresponds to the point of maximum curvature of the reaction path.

the 6-D results. This reflects two facts. First, the molecular vibrational state is a sufficiently good quantum number and is almost conserved during the scattering, i.e., the probability for transitions between different vibrational states during the scattering event is rather low. And second, the curvature of the reaction path of the  $\text{H}_2/\text{Pd}(100)$  PES is not crucial for the vibrational effects in this system because in the 5-D calculations no curvature is present in the Hamiltonian.

As the next step we will analyze the “vibrationally adiabatic potentials” which are defined by

$$V_{\text{adia}}^{\nu_i}(s) = V_0(s) + (\hbar\omega(s) - \hbar\omega_{\text{vib}}) (\nu_i + \frac{1}{2}) , \quad (2)$$

where  $s$  is the coordinate along the reaction path (see Fig. 1). The vibrationally adiabatic potential is the relevant potential for the  $\text{H}_2$  molecule moving on the PES in a particular vibrational state taking the change of the vibrational frequency along the path into account. In Fig. 3 we have plotted the vibrational frequency together with the potential and the vibrational adiabatic potentials for  $\nu_i = 0$  and  $\nu_i = 1$  along the reaction path coordinate  $s$  of Fig. 1. At  $s = 0$ , the point of maximum curvature in Fig. 1, the vibrational frequency is

strongly reduced from its gas phase value of  $\hbar\omega = 516$  meV to about 150 meV. This leads to a lowering of the vibrationally adiabatic potential by 183 meV for  $\nu_i = 0$  and by 549 meV for  $\nu_i = 1$ . Such a lowering does not only occur for the most favorable adsorption path, but also for other non-activated and activated pathways, i.e., for other impact sites in the surface unit cell and for other molecular orientations. This can be demonstrated by the integrated barrier distribution for the potential  $V_0$  and the vibrationally adiabatic potentials

$$P_b(E) = \frac{1}{2\pi A} \int \Theta(E - E_b(\theta, \phi, X, Y)) \cos \theta d\theta d\phi dXdY. \quad (3)$$

In Eq. 3,  $\theta$  and  $\phi$  are the polar and azimuthal orientation of the molecule, and  $X$  and  $Y$  are the lateral coordinates of the hydrogen center-of-mass.  $A$  is the area of the surface unit cell. Each quadruple defines a cut through the six-dimensional space (see Fig. 1 for one example), and  $E_b$  is the minimum energy barrier along such a cut. The function  $\Theta$  is the Heavyside step function. The quantity  $P_b(E)$ , which is plotted in Fig. 4, is the fraction of the configuration space, for which the barrier towards dissociative adsorption is less than  $E$ ; it corresponds to the sticking probability in the classical sudden approximation, which forms the basic approximation behind the so-called “hole model” [31]. Actually, the comparison of Figs. 2 and 4 reveals that the hole model gives a satisfactory description of the sticking probabilities at high kinetic energies above 0.3 eV, whereas it is strongly at variance with full dynamical calculations at low kinetic energies, where the steering effect is operative.

Figure 4 demonstrates that the barrier distribution is lowered due to the decrease of the vibrational frequency by about 180 meV for molecules in the vibrational ground state compared to the potential  $V_0(s)$  and by further  $\approx 400$  meV for molecules in the first excited vibrational state. Because of the lowered potential the vibrationally excited molecules are accelerated more strongly towards the surface, they become so fast that the steering mechanism is suppressed. For that reason the initial decrease of the sticking probability for  $\nu_i = 1$  is limited to low energies ( $E_i \lesssim 50$  meV, see Fig. 2). The difference in the barrier heights of about 400 meV is reflected by the energetic shift between the sticking curves for  $\nu_i = 0$  and  $\nu_i = 1$  in Fig. 2 for sticking probabilities larger than  $\approx 0.7$ . Hence it is the strong decrease of

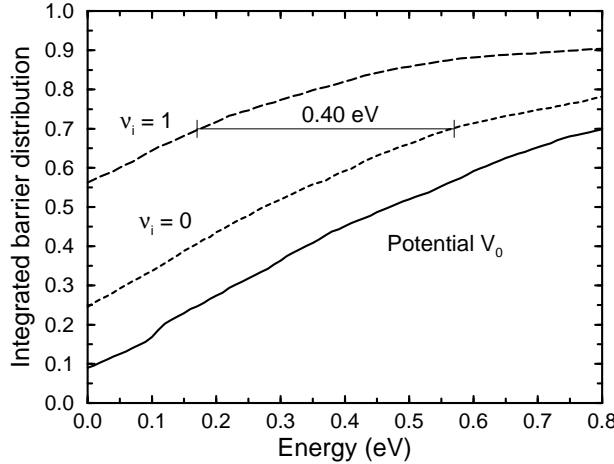


FIG. 4. Integrated barrier distribution using the potential energy  $V_0$  and “vibrationally adiabatic potentials”.

the H-H vibrational frequency during the dissociation which causes the vibrational effects in adsorption.

In figs. 3 and 4 zero-point effects due to the frustrated rotation and translation parallel to the surface are not taken into account since we like to concentrate here on states with different vibrational quantum numbers. The influence of frustrated rotation and translation of the  $H_2$  molecule in contact with the surface will be discussed in a forthcoming paper [32].

According to the principle of detailed balance, the strong enhancement of the sticking probability of vibrationally excited molecules implies a strong vibrational heating of molecules observed in associative desorption. Figure 5 displays the logarithm of the population ratio of the vibrationally first excited and the ground state in desorption versus the inverse surface temperature. The theoretical values were obtained by summing up over all final rotational states. The dashed line results from the assumption that the  $H_2$  vibrations are in thermal equilibrium with the surface temperature. Indeed we find vibrational heating in our calculations. At  $T_s = 700$  K the ratio is 2.5 times higher than for thermal equilibrium. Absolute values of the vibrational heating in hydrogen desorption from Pd(100) were only measured for  $D_2$ , not for  $H_2$ . In the system  $H_2/Ni(110)$ , which has a similar sticking curve as  $H_2/Pd(100)$  [15], a vibrational heating of a factor of two was found [33], in good agreement

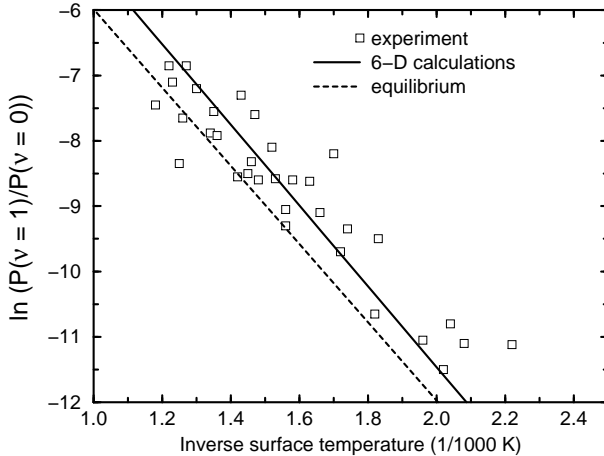


FIG. 5. Vibrational excitation in desorption. Boxes: experimental results (see text) [18]. Dashed line: vibrational population in thermal equilibrium with the surface temperature, solid line: 6-D calculations.

with our results. The experimental results in Fig. 5 are only determined within a calibration factor [18]. This means that only the slope of the experimental data has significance, not the absolute values. From this slope an apparent activation energy  $E_a = 428 \pm 30$  meV [18] has been deduced. Our theoretical work gives  $E_a = 519 \pm 1$  meV. Considering the scatter in the experimental data (see Fig. 5) and the fact that the theory does not employ any empirical parameters, the comparison of the experimentally and theoretically obtained apparent barrier is satisfactory.

In fact, an analysis of the measured sticking probability of H<sub>2</sub>/Pd(100) [15] makes it plausible that the apparent activation energy should be close to the gas-phase frequency of H<sub>2</sub>. If we restrict ourselves for the sake of clarity to the two coordinates  $Z$  and  $d$ , then according to the principle of detailed balance the vibrational population ratio in desorption is given by

$$\frac{P_1}{P_0} = \frac{\int e^{-E/k_B T_s} S(E, \nu_i = 1) dE}{\int e^{-E/k_B T_s} S(E, \nu_i = 0) dE} \cdot \exp\left(\frac{-\hbar\omega_{\text{vib}}}{k_B T_s}\right), \quad (4)$$

where  $S(E, \nu_i)$  is the sticking probability for initial vibrational state  $\nu_i$  and kinetic energy  $E$ . Now an analysis of Eq. 4 yields that a strong lowering of the apparent activation energy from the gas-phase vibrational energy can only be caused by a ratio  $S(E, \nu_i = 1)/S(E, \nu_i = 0)$

which decreases exponentially with increasing kinetic energy. This would only be the case if  $S(E, \nu_i = 0)$  increased exponentially with increasing energy, which requires the assumption of a minimum barrier towards dissociative adsorption, as was done in the calculations of refs. [18,19]. However, the sticking in the system  $H_2/Pd(100)$  is non-activated and initially decreases with increasing kinetic energy [15]. Such a sticking probability should not cause a lowering of the apparent activation energy for vibrational excitation in desorption, as reproduced by our calculations. Either the principle of detailed balance is not directly applicable for the adsorption/desorption of  $H_2/Pd(100)$ , which seems to be improbable from the experience of hydrogen-on-metal systems [3], or there is an inconsistency between the adsorption and desorption experiments.

We further note that the apparent activation energy in our calculations depends on the rotational states of the molecules. If one considers, e.g., only  $j_f = 4$  rotational states, where  $j_f$  is the final rotational quantum number, for the vibrational excitation in desorption, then the theoretical activation energy drops to  $E_a = 487 \pm 2$  meV. This is due to the fact that the sticking probability for molecules in the vibrational ground state becomes small (less than 0.1) for  $j_i \geq 4$  [25], while for vibrationally excited molecules the sticking probability is almost independent of the initial rotational state. Also the absolute value of the vibrational heating depends sensitively on the rotational quantum number; for  $j_f = 4$  the vibrational heating rises to a factor of 3.6.

For  $D_2/Pd(100)$  a vibrational over-population in desorption of  $\nu = 1$  by a factor of nine was found [14], which is much higher than our result for  $H_2/Pd(100)$ . Note that the interaction of  $D_2$  with  $Pd(100)$  is given by *exactly* the same PES as for  $H_2$ . At present, full quantum dynamical calculations for  $D_2$  are not feasible because the number of relevant, energetically accessible channels is significantly higher than for  $H_2$  due to the larger mass and the therefore smaller energetic level spacings. We do not expect, however, that the calculations for  $D_2$  would yield a vibrational heating of a factor of nine. Again analyzing Eq. 4, for such a large vibrational heating the sticking probability for  $\nu_i = 0$  states of  $D_2$  has to be below 0.1 for all energies, much lower than for  $H_2$ , but already the hole model,

that does not take into account the steering effect, yields higher values (see Fig. 4).

The reason for this discrepancy may lie in the determination of the PES. On the other hand, if all experimental results were correct, the application of the principle of detailed balance for the adsorption/desorption of hydrogen/Pd(100) would yield a large isotope effect, which, for example, has not been found for hydrogen on Pd(111) [26]. It may also be that our understanding of the adsorption/desorption dynamics is still incomplete.

### III. CONCLUSIONS

In conclusion, we reported a six-dimensional quantum dynamical study of dissociative adsorption on and associative desorption from H<sub>2</sub>/Pd(100). We have shown that large vibrational effects in dissociative adsorption and associative desorption of H<sub>2</sub>/Pd(100) exist. They are not due to a strongly curved reaction path and a late minimum barrier to adsorption, as was previously assumed, but they are caused by the strong lowering of the H-H vibrational frequency during the adsorption and the multi-dimensionality of the relevant phase space with its broad distribution of barrier heights. Quantitative differences between experiment and theory and inconsistencies between adsorption and desorption experiments are identified which deserve further clarification.

## REFERENCES

- [1] K.D. Rendulic and A. Winkler, *Surf. Sci.* **299/300**, 261 (1994).
- [2] S. Holloway, *Surf. Sci.* **299/300**, 656 (1994).
- [3] G.R. Darling and S. Holloway, *Rep. Prog. Phys.* **58**, 1595 (1995).
- [4] G.D. Kubiak, G.O. Sitz, and R.N. Zare, *J. Chem. Phys.* **83**, 2538 (1985).
- [5] C.T. Rettner, H.A. Michelsen, and D.J. Auerbach, *J. Vac. Sci. Technol. A* **11**, 1901 (1993).
- [6] G. Anger, A. Winkler and K.D. Rendulic, *Surf. Sci.* **220**, 1 (1989).
- [7] B.E. Hayden and C.L.A. Lamont, *Phys. Rev. Lett.* **63**, 1823 (1989).
- [8] C.T. Rettner, D.J. Auerbach, and H.A. Michelsen, *Phys. Rev. Lett.* **68**, 1164 (1992).
- [9] C.T. Rettner, H.A. Michelsen, and D.J. Auerbach, *J. Chem. Phys.* **102**, 4625 (1995).
- [10] B. Jackson and H. Metiu, *J. Chem. Phys.* **86**, 1026 (1987).
- [11] D. Halstead and S. Holloway, *J. Chem. Phys.* **93**, 2859 (1990).
- [12] S. Küchenhoff, W. Brenig, and Y. Chiba, *Surf. Sci.* **245**, 389 (1991).
- [13] G.R. Darling and S. Holloway, *J. Chem. Phys.* **97**, 734 (1992).
- [14] L. Schröter, H. Zacharias, and R. David, *Phys. Rev. Lett.* **62**, 571 (1989).
- [15] K. D. Rendulic, G. Anger, and A. Winkler, *Surf. Sci.* **208**, 404 (1989).
- [16] L. Schröter, Chr. Trame, R. David, and H. Zacharias, *Surf. Sci.* **272**, 229 (1992).
- [17] S. Wilke and M. Scheffler, *Surf. Sci.* **329**, L605 (1995); *Phys. Rev. B*, in press.
- [18] L. Schröter, S. Küchenhoff, R. David, W. Brenig, and H. Zacharias, *Surf. Sci.* **261** (1992) 243.
- [19] W. Brenig and R. Russ, *Surf. Sci.* **315**, 195 (1994).

- [20] G.R. Darling and S. Holloway, *Surf. Sci.* **268**, L305 (1992).
- [21] G. R. Darling, *Faraday Discuss. Chem. Soc.* **96**, 87 (1993).
- [22] W. Brenig, T. Brunner, A. Gross, and R. Russ, *Z. Phys. B* **93**, 91 (1993).
- [23] A. Gross, S. Wilke, and M. Scheffler, *Phys. Rev. Lett.* **75**, 2718 (1995).
- [24] M. Kay, G.R. Darling, S. Holloway, J.A. White, and D.M. Bird, *Chem. Phys. Lett.* **245**, 311 (1995).
- [25] A. Gross, S. Wilke, and M. Scheffler, *Surf. Sci.*, in press.
- [26] M. Beutl, M. Riedler, and K.D. Rendulic, *Chem. Phys. Lett.* **247**, 249 (1995)
- [27] D. Wetzig, R. Dopheide, M. Rutkowski, R. David, and H. Zacharias, *Phys. Rev. Lett.* **76**, 463 (1996).
- [28] G.R. Darling and S. Holloway, *J. Chem. Phys.* **93** (1990) 9145.
- [29] A. Gross, *J. Chem. Phys.* **102**, 5045 (1995).
- [30] J.B. Pendry, *Low energy electron diffraction*, Academic Press, London (1974).
- [31] M. Karikorpi, S. Holloway, N. Henriksen and J.K. Nørskov, *Surf. Sci.* **179**, L41 (1987).
- [32] A. Gross and M. Scheffler, to be published.
- [33] A. Winkler, G. Eilmsteiner, and R. Novak, *Chem. Phys. Lett.* **226**, 589 (1994).